The Astrophysical Journal Letters, 885:L10 (6pp), 2019 November 1 https://doi.org/10.3847/2041-8213/ab4da8
© 2019. The American Astronomical Society. All rights reserved.

Detection of Pulses from the Vela Pulsar at Millimeter Wavelengths with Phased ALMA

Kuo Liu[1], André Young[2], Robert Wharton[1], Lindy Blackburn[3,4], Roger Cappallo[5], Shami Chatterjee[6], James M. Cordes[6], Geoffrey B. Crew[7], Gregory Desvignes[1,8], Sheperd S. Doeleman[3,4], Ralph P. Eatough[1], Heino Falcke[2], Ciriaco Goddi[2,9], Michael D. Johnson[3,4], Simon Johnston[10], Ramesh Karuppusamy[1], Michael Kramer[1], Lynn D. Matthews[7], Scott M. Ransom[11], Luciano Rezzolla[12], Helge Rottmann[1], Remo P. J. Tilanus[2,9,13], and Pablo Torne[1,14]

[1] Max-Planck-Institut für Radioastronomie, Auf dem Hügel 69, D-53121 Bonn, Germany; kliu@mpifr-bonn.mpg.de
[2] Department of Astrophysics, Institute for Mathematics, Astrophysics and Particle Physics (IMAPP), Radboud University, P.O. Box 9010, 6500 GL Nijmegen, The Netherlands
[3] Center for Astrophysics|Harvard & Smithsonian, 60 Garden Street, Cambridge, MA 02138, USA
[4] Black hole Initiative at Harvard University, 20 Garden Street, Cambridge, MA 02138, USA
[5] Massachusetts Institute of Technology Haystack Observatory, 99 Millstone Road, Westford, MA 01886, USA
[6] Cornell Center for Astrophysics and Planetary Science, Cornell University, Ithaca, NY 14853, USA
[7] Massachusetts Institute of Technology Haystack Observatory, 99 Millstone Road, Westford, MA 01886, USA
[8] LESIA, Observatoire de Paris, Université PSL, CNRS, Sorbonne Université, Université de Paris, 5 place Jules Janssen, F-92195 Meudon, France
[9] Leiden Observatory—Allegro, Leiden University, P.O. Box 9513, 2300 RA Leiden, The Netherlands
[10] CSIRO Astronomy and Space Science, Australia Telescope National Facility, P.O. Box 76, Epping, NSW 1710, Australia
[11] National Radio Astronomy Observatory, Charlottesville, VA 22903, USA
[12] Institut für Theoretische Physik, Goethe-Universität Frankfurt, Max-von-Laue-Straße 1, D-60438 Frankfurt am Main, Germany
[13] Netherlands Organisation for Scientific Research (NWO), Postbus 93138, 2509 AC Den Haag, The Netherlands
[14] Instituto de Radioastronomía Milimétrica, IRAM, Avenida Divina Pastora 7, Local 20, E-18012, Granada, Spain
Received 2019 August 6; revised 2019 October 11; accepted 2019 October 14; published 2019 October 29

Abstract

We report on the first detection of pulsed radio emission from a radio pulsar with the Atacama Large Millimeter/submillimeter Array (ALMA) telescope. The detection was made in the Band-3 frequency range (85–101 GHz) using ALMA in the phased-array mode developed for VLBI observations. A software pipeline has been implemented to enable a regular pulsar observing mode in the future. We describe the pipeline and demonstrate the capability of ALMA to perform pulsar timing and searching. We also measure the flux density and polarization properties of the Vela pulsar (PSR J0835–4510) at millimeter wavelengths, providing the first polarimetric study of any ordinary pulsar at frequencies above 32 GHz. Finally, we discuss the lessons learned from the Vela observations for future pulsar studies with ALMA, particularly for searches near the supermassive black hole in the Galactic center, and the potential of using pulsars for polarization calibration of ALMA.

Unified Astronomy Thesaurus concepts: Interferometry (808); Pulsars (1306); Millimeter astronomy (1061)

1. Introduction

Pulsars are steep-spectrum radio sources (e.g., Lorimer & Kramer 2005). As a result, the vast majority of the pulsar population have been discovered at frequencies below 2 GHz. Correspondingly, the study of the radio emission has been limited to similar frequencies, although successful studies have been conducted up to much higher frequencies. Before 1990, the highest frequency used for successful pulsar studies was 25 GHz, while in the 1990s observations were pushed to 32 GHz (Wielebinski et al. 1993), 43 GHz (Kramer et al. 1997), and finally 87 GHz (Morris et al. 1997). Emission from normal pulsars was later observed at 138 GHz (Torne 2016), and finally, detections of the radio-emitting magnetar PSR J1745−2900 were achieved at frequencies as high as 291 GHz (for a review, see Torne 2018).

Observations at high frequencies will provide a better understanding of pulsar emission physics and allow for more effective pulsar searches in highly turbulent environments like the Galactic center (Cordes & Lazio 1997; Lorimer & Kramer 2005; Spitler et al. 2014; Dexter et al. 2017). Previous pulsar studies have suggested that the coherent emission seen at lower radio frequencies may undergo changes at high radio frequencies (Kramer et al. 1996). This may be understood as a breakdown of the coherent radiation mechanism, which can be expected to occur when the observed wavelength becomes comparable to the coherence length. The breakdown would correspond to a transition from the coherent radio emission to the incoherent infrared or optical emission (Lorimer & Kramer 2005). At the same time, a standard model of pulsar emission physics interprets observed pulse characteristics as the result of a "radius-to-frequency mapping," where higher radio frequencies are emitted from lower emission heights (Cordes 1978). In the context of this model, performing observations at higher radio frequencies is equivalent to approaching the polar cap region of the pulsar.

All previous studies of pulsars above 30 GHz have been conducted with northern hemisphere radio telescopes, especially the 100 m Effelsberg radio telescope near Bonn, Germany, and the 30 m telescope of the Institut de Radioastronomie Millimétrique on Pico Veleta, Spain (see Löhmer et al. 2008 and Torne et al. 2017 and references therein). With the advent of the Atacama Large Millimeter/submillimeter Array (ALMA), a large collecting area is now available to study southern hemisphere pulsars. Here we report on the establishment of a fast time-domain capability (hereafter a "pulsar observing mode") for ALMA's phased-array system (Matthews et al. 2018). This new pulsar observing mode can be used for observations of compact objects in the Galactic center

and elsewhere in the Galaxy. We demonstrate the capabilities of this system with observations of the Vela pulsar.

As one of the brightest radio pulsars in the sky, Vela was one of the first pulsars discovered (Large et al. 1968) despite its relatively fast spin period ($P_{\rm spin} = 89$ ms). Recently, an imaging detection of Vela was made at millimeter wavelengths using ALMA in its standard interferometry observing mode (Mignani et al. 2017). As shown below, we can now use phased ALMA (i.e., ALMA in the phased-array mode) to obtain a complementary study of Vela's pulsed and polarized emission at frequencies of 90 GHz and above.

ALMA can also play a key role in probing neutron star populations in the Galactic center and using detected objects for the study of spacetime around the central black hole, the Sgr A* (Liu et al. 2012; Psaltis et al. 2016; Liu & Eatough 2017). Despite previous efforts, no pulsar in a sufficiently close orbit to Sgr A* has yet been detected (Wharton et al. 2012). However, the discovery of a rare radio-emitting magnetar (PSR J1745−2900) with a projected distance of only ≈0.1 pc from the Sgr A* (Eatough et al. 2013) suggests the existence of an intrinsic pulsar population in the immediate vicinity of Sgr A*. PSR J1745−2900 has been studied up to frequencies of 291 GHz (Torne et al. 2017), indeed implying that ALMA will be an ideal instrument to study its properties.

The development project described here (the ALMA Pulsar Mode Project, hereafter APMP) involves a series of steps needed to acquire phased ALMA data for pulsar studies: definition and implementation of the appropriate phasing mode, providing the signal path from the ALMA Phasing Project (APP) system to Mark 6 baseband recorders, offline resampling and reformatting of data into PSRFITS format (Hotan et al. 2004), and development of the backend pulsar/transient processing customized to ALMA science contexts. The project leveraged software development for pulsar phased-array modes for the Very Large Array[15] and developments for the Event Horizon Telescope (Doeleman et al. 2008; Event Horizon Telescope Collaboration et al. 2019), black hole Camera (Goddi et al. 2017) projects, and the APP (Matthews et al. 2018).

2. Observations

Feasibility studies conducted for the APMP used test data obtained in conjunction with APP commissioning runs in 2016 April and 2017 January. The former provided data used to test the integrity of the Mark 6 to PSRFITS transformation while the latter provided data on the Vela pulsar (PSR J0835−4510) for validation purposes. Detection of the pulsar at a significance consistent with the sensitivity (A/T) and bandwidth used was the primary goal in order to demonstrate the feasibility of pulsar and transient observations with ALMA. Demonstrating the ability to use pulsar observations for system tests and instrumental polarization calibration were secondary goals. Finally, comparing the properties of the Vela pulse profile with those obtained at lower frequencies allows us to study pulsar emission physics.

The observation of the Vela pulsar was conducted with ALMA using Band-3 on 2017 January 29 under excellent weather conditions. The observation spanned approximately

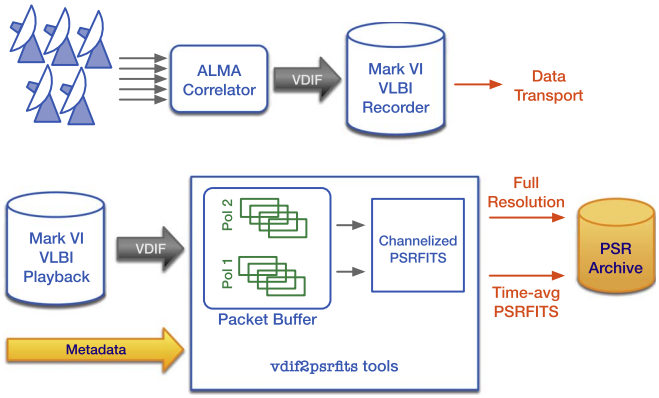

Figure 1. Developed ALMA system for offline processing to produce pulsar/transients data. The phased ALMA voltage data are recorded on Mark6 VLBI recorders (Whitney et al. 2013). In our study the data were played back and processed at Cornell University, the Massachusetts Institute of Technology (MIT) Haystack Observatory, the Center for Astrophysics | Harvard & Smithsonian (CfA), and the Max Plank Institut für Radioastronomie (MPIfR) to produce PSRFITS format pulsar data (https://www.atnf.csiro.au/research/pulsar/psrfits_definition/Psrfits.html). The box represents the software suites that convert VDIF format data into PSRFITS data, and are publicly available on http://hosting.astro.cornell.edu/research/almapsr/. As described there, two pipelines of such have been developed independently at MPIfR and CfA.

40 minutes. In total, 37 12 m antennas were phased up to form a tied-array beam, delivering a collecting area equivalent to a 73 m parabolic dish. The entire observation was divided into eight individual scans where the telescope was alternately pointed at Vela and a bright neighboring phase calibrator (J0828−3731, 0.87 Jy measured on 2015 December 25 and 8° separation). "Active phasing" mode was deployed during the calibrator scans, where the phasing solution was updated every 18.192 s. During the scans on the Vela pulsar, the latest phasing solution from the last calibrator scan was adopted and kept unchanged (the so-called "passive phasing" mode). During the observation, the baseband data streams from two sidebands (each consisting of two subbands) were recorded, providing 4 × 2 GHz subbands centered at 86.268, 88.268, 98.268, and 100.268 GHz, respectively. Each subband was subdivided into 32 × 62.5 MHz frequency channels. The data were then processed offline to yield intensity detections for all Stokes parameters with a time resolution of 8 μs and packed in PSRFITS format in search mode (channelized time series). For the purpose of detecting the Vela pulsar, the data were folded to form 10 s subintegrations, using an ephemeris obtained from low-frequency observations around the same period of time. Details on the data flow and the preprocessing can be found in Figure 1.

3. Results

The Vela pulsar has been successfully detected after folding the search mode data. Figure 2 shows the integrated pulse profiles obtained from the lower and upper sideband, respectively. An effective integration time of 25 minutes yields a peak signal-to-noise ratio of the detection of ∼50 for the lower and ∼40 for the upper sideband. The signal was detected at frequencies up to 101.268 GHz, the highest radio frequency at which the pulse profile of Vela has ever been seen. Overall, the ALMA detection of the Vela pulsar provides a successful demonstration of the APMP and provides the basis for future execution of our primary scientific motivation: searches and

[15] https://science.nrao.edu/facilities/vla/docs/manuals/oss/performance/pulsar

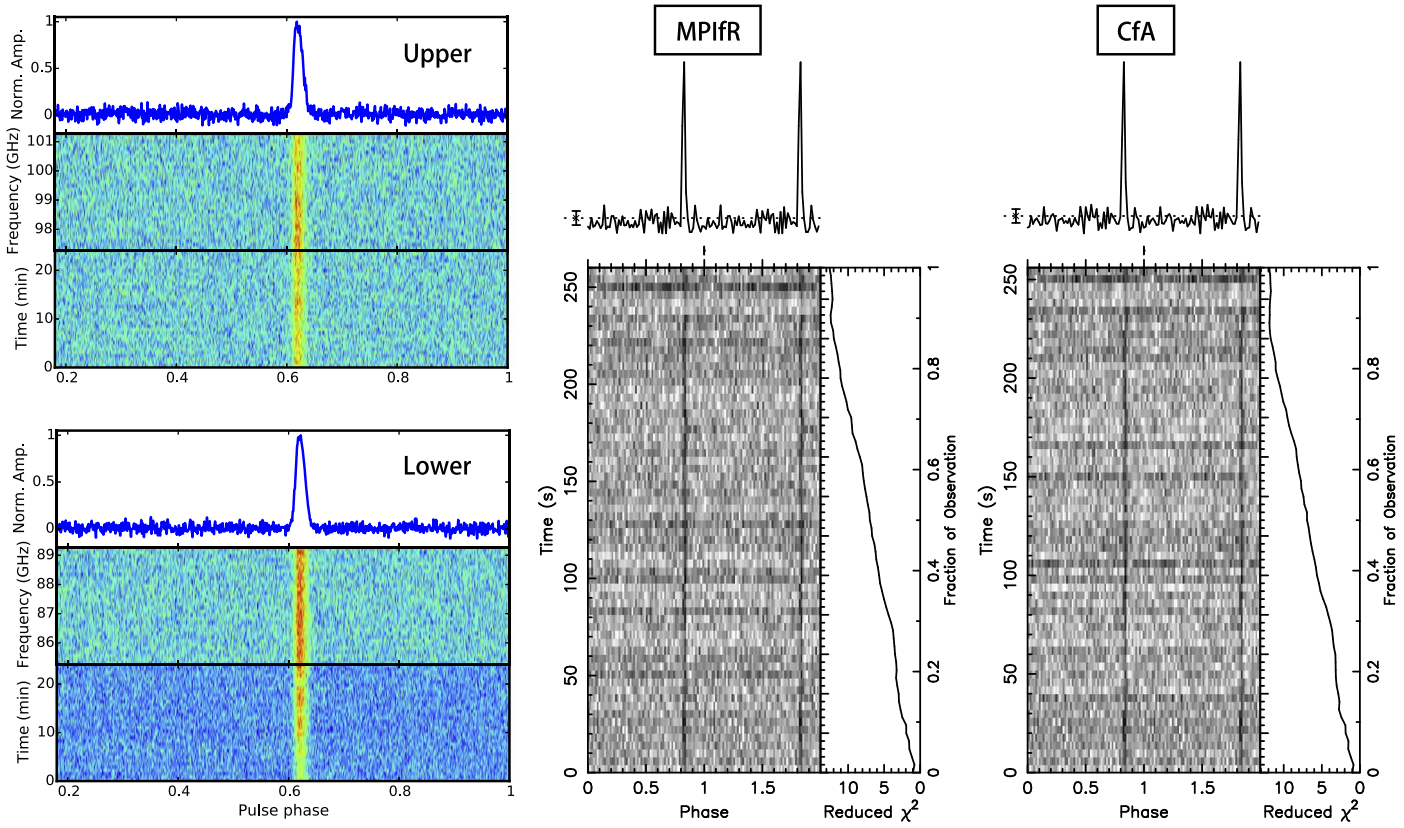

Figure 2. Left panel: pulse profiles detected in the lower (bottom, 85.268–89.268 GHz) and upper sideband (top, 96.268–101.268 GHz) of ALMA Band-3, using the MPIfR pipeline. Middle and right panel: comparison of pulse profile achieved from the MPIfR and CfA pipeline (folded using the PRESTO software package; Ransom et al. 2002). In short, the MPIfR pipeline makes power detection of all four Stokes parameters in frequency domain, while the CfA pipeline derives total intensity power directly from the state counts. With the same section of data, the detection from these two pipelines shows highly consistent measures of detection significance in total intensity and the shape of the pulse profile of the Vela pulsar. The product from the MPIfR pipeline is used for the data analysis in the rest of this paper.

follow-up observations of pulsars and transient sources in the Galactic center.

3.1. Timing

The utility of pulsars as precision clocks, the so-called pulsar timing technique, requires high timing stability during the process of data recording. To examine such a capability of the phased ALMA data, we carried out a timing analysis with the 10 s subintegrations from both sidebands. For each of them, we averaged the pulse profile over frequency, and calculated its time of arrival (TOA) with the canonical template-matching method (Taylor 1992). Figure 3 shows the timing residuals obtained by subtracting the predictions of the ephemeris (obtained independently from low-frequency observations) from the TOAs. No time offset was seen between the four individual scans. A weighted root-mean-square timing uncertainty of 134 μs has been achieved, which is in general consistent with the TOA errors expected from radiometer noise. This shows that a timing precision of order 100 μs that was used in the simulation of Liu et al. (2012), is in fact possible for pulsar observations with ALMA at 3 mm wavelengths.

3.2. Search Capability

To demonstrate the capability of the APMP for searching for periodic signals in the data, we used the overall data set to directly carry out a blind search for the Vela pulsar. We first averaged the time series from all four individual subbands for each scan, and combined the time series from all four scans,

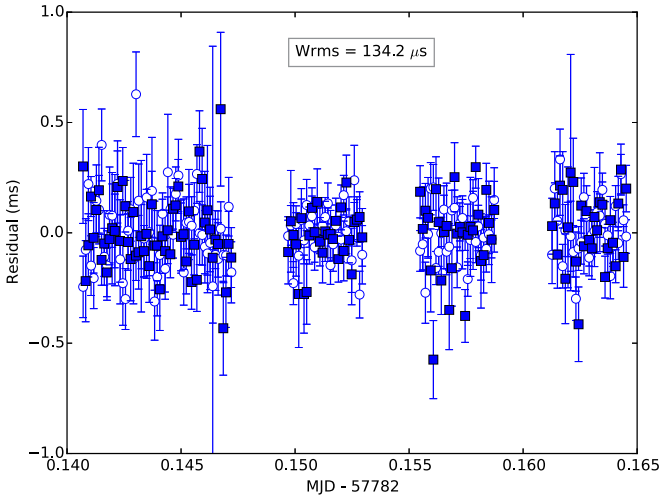

Figure 3. Timing residuals of Vela pulse profiles derived from 10 s subintegrations. The open circles and squares represent residuals from the lower and upper sidebands, respectively.

with the power mean padded in the gaps among the scans. Then a periodicity search was performed using the PRESTO[16] software package (Ransom et al. 2002). Figure 4 shows the power spectrum of the combined time series. The low-frequency noise, mainly caused by fluctuations of the power level in the time series, starts to become significant for

[16] https://www.cv.nrao.edu/~sransom/presto/

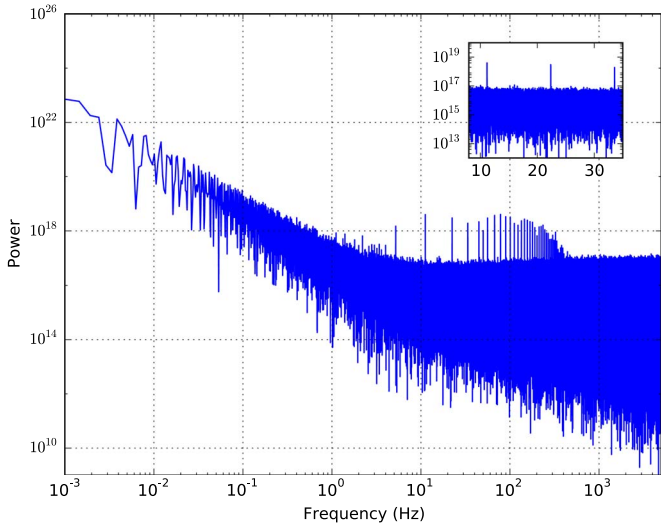

Figure 4. Fourier power spectrum of the overall time series formed by combining data from all four individual Vela scans. For each scan, the time series was first averaged in frequency. The inset shows a zoomed-in region of the power spectrum for frequencies between 5 and 35 Hz, with linear scale on the x-axis. Note that the spinning frequency of the Vela pulsar is approximately 11.2 Hz.

frequencies below 5 Hz. Meanwhile, the overall power level of the rest of the spectrum is mostly flat. The fundamental spinning frequency of the Vela pulsar (around 11.2 Hz) and its higher order harmonics are clearly seen in the Figure 4 inset. The periodicity search resulted in 28 candidates with detection significance above 3σ. The fundamental spin frequency of the Vela pulsar was the top candidate and most of the rest were higher harmonics. At frequencies of 50 and 1 Hz, periodic signals were detected and associated with the electricity power cycle and cryogenic pump's cycle, respectively. Another signal was detected at 2.6 Hz, and its origin is unknown but is likely to be terrestrial, as it was also seen in scans of the calibrator.[17]

3.3. Pulsar Properties

We can use the obtained data to study the properties of the Vela pulsar at frequencies between 80 and 100 GHz and compare those to Vela's properties at lower frequencies, and to those of PSR B0355+54 (to be presented in future work), the only other normal pulsar detected at similar frequencies (Morris et al. 1997; Torne 2016). This will allow us to gauge the prospects of future pulsar observations with ALMA and further our understanding of pulsar emission physics.

3.3.1. Flux Density

The recorded data of the phase calibrator J0828−3731 allow us to estimate the mean flux density of the Vela pulsar profile. For each individual scan we produced imaging detection of the phase calibrator and measured its flux density at the lower and upper sidebands, respectively, which gave consistent values with those from the ALMA calibrator catalog.[18] Then for each individual Vela scan, we used the closest calibrator scan to calibrate the flux density of the pulsed emission, by using the standard flux calibration formula (Lorimer & Kramer 2005).

[17] The ALMA baseline correlator is clocked (precisely) at 125 MHz with microprocessor interrupts at 16 ms and timing signals at 48 ms—so signals commensurate with these are likely to have been produced in the correlator.
[18] https://almascience.nrao.edu/sc/

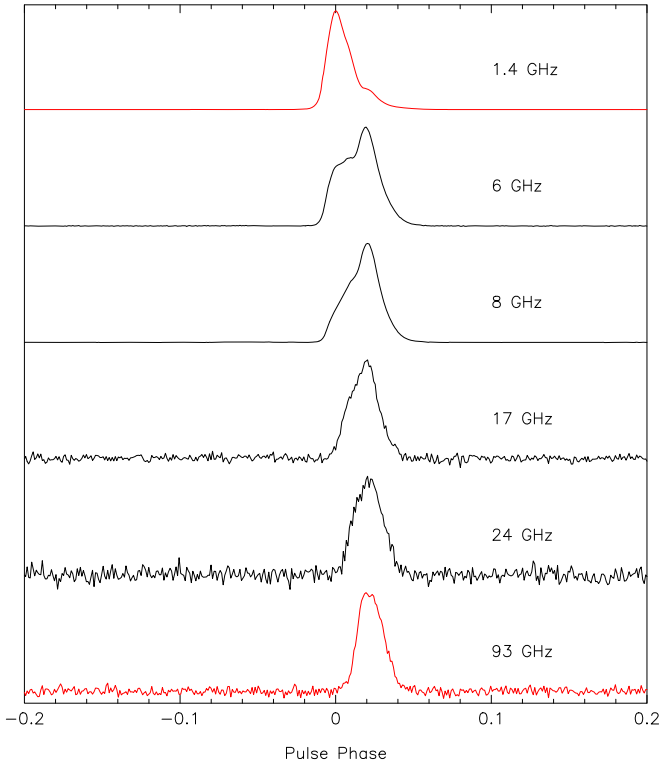

Figure 5. Vela profiles measured as a function of frequency. The bottom profile (red) is the result of the addition of the two ALMA sidebands. It is aligned in time, using the data's timestamps, with the 1.4 GHz profile shown on top (red), which resulted from an observation with the Parkes Radio Telescope at 1.4 GHz made on 2017 January 8. Note that using nearly contemporaneous observations with Parkes, we minimize any confusing time delay potentially caused by rotational instabilities known as "timing noise." Indeed, the apparent delay of 1.8 ms of the ALMA profile with respect of the pulse peak seen at 1.4 GHz can be explained by a distinct profile evolution. This becomes clear when adding the profiles (black) observed and aligned by Keith et al. (2011). See the text for details.

This gave us a mean flux density of 0.99 ± 0.17 mJy and 0.69 ± 0.12 mJy at 87.268 and 99.268 GHz, respectively, where the error bars represent the actual standard deviation of all four individual measurements. Using the ordinary ALMA interferometry data recorded in parallel during the observation and calibrated following the dedicated procedures developed for phased ALMA (Goddi et al. 2019), we also produced image detections of the Vela pulsar from all individual scans, which delivered mean flux density measurements of 0.82 ± 0.09 mJy and 0.67 ± 0.05 mJy at 87.268 and 99.268 GHz, respectively. These are fully consistent with the measurements derived from the phased ALMA data.

3.3.2. Profile Evolution

The lack of a drift during the folding of the data (see Figure 2) and the apparent timing stability (Section 3.1) imply that the data timestamps are reliable. Going further, we can compare the phase of the pulse arrival time at 1.4 GHz (obtained at the Parkes Radio Telescope), defined by that of the main pulse peak (identified with phase zero), with that of the pulse peak seen with ALMA at millimeter wavelengths. Figure 5 demonstrates that the latter is delayed by about 1.8 ms with respect to the main pulse peak at 1.4 GHz. This offset is explained by comparing the profiles to those at intermediate frequencies. We use those presented by Keith

et al. (2011), following their alignment based on a separation of the profile into individual components.[19] As can be seen from Figure 5 the main component seen at 1.4 GHz (and below) becomes progressively weaker at high frequencies and is undetectable at ALMA frequencies. The component remaining is the second, weaker component of the 1.4 GHz profile. This is consistent with the identification of the dominant 1.4 GHz component seen in the top profile of Figure 5, with a so-called "core component" (see, e.g., Johnston et al. 2001) which tends to have steeper spectra. Indeed, Keith et al. (2011) measure a spectral index of -2.7 ± 0.1 for this component, compared to -1.5 ± 0.2 for the component seen with ALMA.[20] Extrapolating from the 24 GHz flux density (3.4 mJy, Keith et al. 2011), we therefore expect a flux density of 0.94 ± 0.14 mJy at 87 GHz and 0.82 ± 0.31 mJy at 99 GHz. This is in perfect agreement with the flux density measurement we obtained (see Section 3.3.1).

3.3.3. Polarization Properties

The MPIfR pipeline allows for the extraction of full-Stokes information from ALMA baseband data. We find that Vela still shows some significant linear and circular polarization. Assuming that the observed polarization characteristics are similar to those observed at 24 GHz, we can use the data by Keith et al. (2011) as a polarization template and perform a system calibration without needing to make any assumptions on "ideal feeds" or additional constraints on degeneracy in the system parameters[21] (van Straten 2006; Smits et al. 2017). The result is shown in Figure 6, where we show an expanded region around the pulse. Here, the degree of linear polarization (~20%) is lower than at 24 GHz but the position angle is perfectly consistent with the 1.4 GHz data (after correcting for Faraday rotation). This change in degree of polarization, while maintaining a constant PA swing (believed to be tied to the magnetic field and the viewing geometry of the pulsar), is perfectly consistent with overall trends in other pulsars (Lorimer & Kramer 2005). The sign of circular polarization is identical to that at lower frequencies and its fraction relative to total intensity is similar to that at 24 GHz.

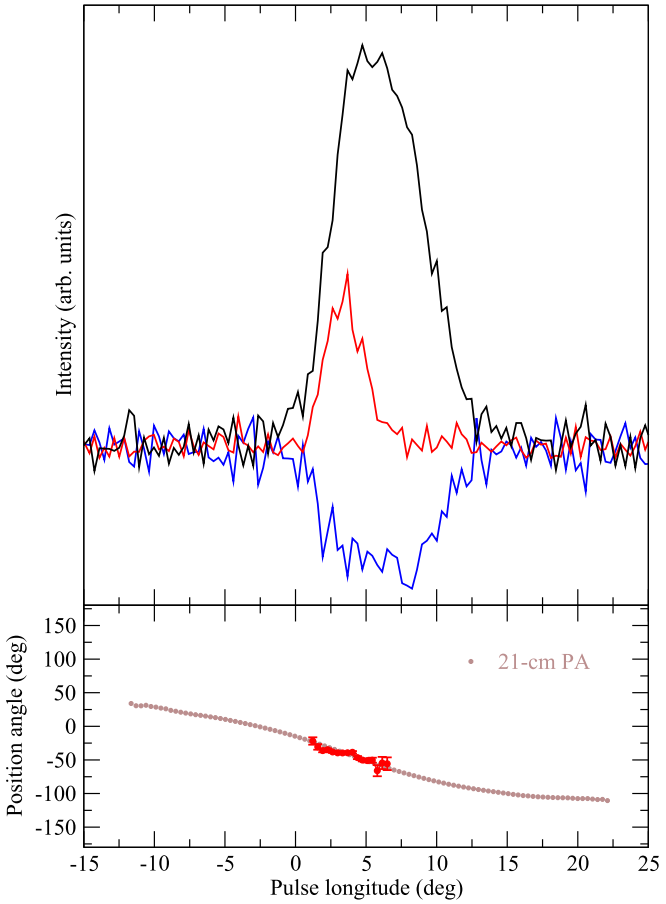

Figure 6. Polarization properties of the Vela pulsar as observed with ALMA, when adding the Stokes vectors measured for the lower and upper sidebands. The top panel shows the total power (black), the linearly polarized emission component (red), and the circularly polarized emission (blue). The lower panel shows the position angle of the linearly polarized component as a function of those pulse phases, where the linear intensity exceeds 1.5σ of the off-pulse region. We also indicated the position angle swing measured at 1.4 GHz, corrected for Faraday rotation to infinite frequency.

4. Discussion

We have demonstrated the capability of phased ALMA for the study of pulsars. The use of phased ALMA in combination with a passive phasing mode will enable future pulsar searches, as well as timing, polarization, and emission studies. This opens up new scientific possibilities, especially in the southern hemisphere, which is completely unexplored for pulsars at frequencies above 30 GHz.

Given the typical steep spectrum of pulsars, they will generally be far too weak at ALMA frequencies to allow active phasing of the ALMA array on the pulsar itself. The periodicity search experiment carried out in this paper used a passive phasing mode. Our results demonstrate the high data quality that can be achieved using this mode of phased ALMA for pulsar studies. Meanwhile, in the data collected in active phasing scans on a bright calibrator source, we noticed significant systematics in the time series which are associated with the phasing cycles. This issue will be investigated further in a forthcoming paper. This means that it will be highly preferable for future pulsar observations with phased ALMA to be conducted in passive phasing mode, irrespective of the flux density of the source.

As shown in our analysis, it is possible to use a pulsar as a calibrator to understand and calibrate the polarization of phased ALMA data. In particular, because the Vela pulsar exhibits apparent circular polarization at 3 mm wavelengths, it could potentially help to better estimate the leakages in a linear feed system. Additionally, the low rotation measure of this pulsar RM = 31.4 rad m^{-2} (Johnston et al. 2005) guarantees that the contamination by Faraday rotation during the calibration process is negligible at 3 mm wavelengths. To carry out this experiment, a long track of the Vela pulsar needs to be conducted in order to cover a wide range of parallactic angles. Then a calibration can be performed by following the approach

[19] Keith et al. (2011) modeled the profiles at different frequencies as a sum of a number of symmetric components represented by scaled von Mises functions. They found that a set of the same four component fits to all frequencies while keeping the width and separation of each component fixed. We aligned their solution relative to our ALMA and Parkes observations by eye.

[20] Note that we identify Keith et al.'s (2011) component C and/or D with the ALMA component, for which a spectral index of -1.56 ± 0.06 and -1.5 ± 0.2 was determined, respectively. We adopt -1.5 with its larger uncertainty here.

[21] Here we chose only to fit for differential gain and phase, as the leakage in ALMA Band-3 was shown to be no more than a few percent (Goddi et al. 2019).

described in van Straten (2004, 2006), after which a polarization template of the Vela pulsar at the given frequency will be constructed. For calibration afterwards, one would only need a short scan on the Vela pulsar and match it to the template.

We thank A. Evans, T. Remijan, and F. Stoehr for the help to stage our data on the ALMA science portal.[22] K.L., R.W., G. D., R.P.E., H.F., C.G., M.K., L.R., and P.T. acknowledge the financial support by the European Research Council for the ERC Synergy grant BlackHoleCam under contract No. 610058. S.C. and J.M.C. acknowledges support from the National Science Foundation (AAG 1815242). Work on this project at the Smithsonian Astrophysical Observatory was funded by NSF grant AST-1440254. This paper makes use of the following ALMA data: ADS/JAO.ALMA#2011.0.00004.E. ALMA is a partnership of ESO (representing its member states), NSF (USA) and NINS (Japan), together with NRC (Canada), *MOST*, and ASIAA (Taiwan), and KASI (Republic of Korea), in cooperation with the Republic of Chile. The Joint ALMA Observatory is operated by ESO, AUI/NRAO, and NAOJ. The National Radio Astronomy Observatory is a facility of the National Science Foundation operated under cooperative agreement by Associated Universities, Inc. The ALMA Phasing Project was principally supported by a Major Research Instrumentation award from the National Science Foundation (award 1126433) and an ALMA North American Development Augmentation award to Cornell University; the ALMA Pulsar Mode Project was supported by an ALMA North American Study award.

Facility: ALMA.

Software: PRESTO.

ORCID iDs

Kuo Liu https://orcid.org/0000-0002-2953-7376
André Young https://orcid.org/0000-0003-0000-2682
Robert Wharton https://orcid.org/0000-0002-7416-5209
Lindy Blackburn https://orcid.org/0000-0002-9030-642X
Shami Chatterjee https://orcid.org/0000-0002-2878-1502
James M. Cordes https://orcid.org/0000-0002-4049-1882
Geoffrey B. Crew https://orcid.org/0000-0002-2079-3189
Gregory Desvignes https://orcid.org/0000-0003-3922-4055
Sheperd S. Doeleman https://orcid.org/0000-0002-9031-0904
Ralph P. Eatough https://orcid.org/0000-0001-6196-4135
Heino Falcke https://orcid.org/0000-0002-2526-6724
Michael D. Johnson https://orcid.org/0000-0002-4120-3029
Simon Johnston https://orcid.org/0000-0002-7122-4963
Ramesh Karuppusamy https://orcid.org/0000-0002-5307-2919
Michael Kramer https://orcid.org/0000-0002-4175-2271
Lynn D. Matthews https://orcid.org/0000-0002-3728-8082
Scott M. Ransom https://orcid.org/0000-0001-5799-9714
Luciano Rezzolla https://orcid.org/0000-0002-1330-7103
Remo P. J. Tilanus https://orcid.org/0000-0002-6514-553X
Pablo Torne https://orcid.org/0000-0001-8700-6058

[22] The data are available via: https://almascience.eso.org/alma-data/enhanced-data-products/vela-pulsar-j0835-4510.

References

Cordes, J. M. 1978, ApJ, 222, 1006
Cordes, J. M., & Lazio, J. T. W. 1997, ApJ, 475, 557
Dexter, J., Deller, A., Bower, G. C., et al. 2017, MNRAS, 471, 3563
Doeleman, S. S., Weintroub, J., Rogers, A. E. E., et al. 2008, Natur, 455, 78
Eatough, R. P., Falcke, H., Karuppusamy, R., et al. 2013, Natur, 501, 391
Event Horizon Telescope Collaboration, Akiyama, K., Alberdi, A., et al. 2019, ApJL, 875, L2
Goddi, C., Falcke, H., Kramer, M., et al. 2017, IJMPD, 26, 1730001
Goddi, C., Martí-Vidal, I., Messias, H., et al. 2019, PASP, 131, 075003
Hotan, A. W., van Straten, W., & Manchester, R. N. 2004, PASA, 21, 302
Johnston, S., Hobbs, G., Vigeland, S., et al. 2005, MNRAS, 364, 1397
Johnston, S., van Straten, W., Kramer, M., & Bailes, M. 2001, ApJL, 549, L101
Keith, M. J., Johnston, S., Levin, L., & Bailes, M. 2011, MNRAS, 416, 346
Kramer, M., Jessner, A., Doroshenko, O., & Wielebinski, R. 1997, ApJ, 488, 364
Kramer, M., Xilouris, K. M., Jessner, A., Wielebinski, R., & Timofeev, M. 1996, A&A, 306, 867
Large, M. I., Vaughan, A. E., & Mills, B. Y. 1968, Natur, 220, 340
Liu, K., & Eatough, R. 2017, NatAs, 1, 812
Liu, K., Wex, N., Kramer, M., Cordes, J. M., & Lazio, T. J. W. 2012, ApJ, 747, 1
Löhmer, O., Jessner, A., Kramer, M., Wielebinski, R., & Maron, O. 2008, A&A, 480, 623
Lorimer, D. R., & Kramer, M. 2005, Handbook of Pulsar Astronomy (Cambridge: Cambridge Univ. Press)
Matthews, L. D., Crew, G. B., Doeleman, S. S., et al. 2018, PASP, 130, 015002
Mignani, R. P., Paladino, R., Rudak, B., et al. 2017, ApJL, 851, L10
Morris, D., Kramer, M., Thum, C., et al. 1997, A&A, 322, L17
Psaltis, D., Wex, N., & Kramer, M. 2016, ApJ, 818, 121
Ransom, S. M., Eikenberry, S. S., & Middleditch, J. 2002, AJ, 124, 1788
Smits, R., Bassa, C. G., Janssen, G. H., et al. 2017, A&C, 19, 66
Spitler, L. G., Lee, K. J., Eatough, R. P., et al. 2014, ApJL, 780, L3
Taylor, J. H. 1992, RSPTA, 341, 117
Torne, P. 2016, PhD thesis, Bonn Univ.
Torne, P. 2018, in IAU Symp. 337, Pulsar Astrophysics the Next Fifty Years, ed. P. Weltevrede (Cambridge: Cambridge Univ. Press), 92
Torne, P., Desvignes, G., Eatough, R. P., et al. 2017, MNRAS, 465, 242
van Straten, W. 2004, ApJ, 152, 129
van Straten, W. 2006, ApJ, 642, 1004
Wharton, R. S., Chatterjee, S., Cordes, J. M., Deneva, J. S., & Lazio, T. J. W. 2012, ApJ, 753, 108
Whitney, A. R., Beaudoin, C. J., Cappallo, R. J., et al. 2013, PASP, 125, 196
Wielebinski, R., Jessner, A., Kramer, M., & Gil, J. A. 1993, A&A, 272, L13